

## Accepted Manuscript

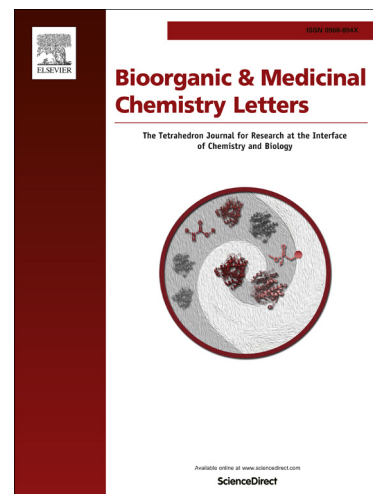
Aryl-substituted aminobenzimidazoles targeting the hepatitis C virus internal ribosome entry site

Kejia Ding, Annie Wang, Mark A. Boerneke, Sergey M. Dibrov, Thomas Hermann

PII: S0960-894X(14)00496-X  
DOI: <http://dx.doi.org/10.1016/j.bmcl.2014.05.009>  
Reference: BMCL 21622

To appear in: *Bioorganic & Medicinal Chemistry Letters*

Received Date: 7 January 2014  
Revised Date: 1 May 2014  
Accepted Date: 5 May 2014



Please cite this article as: Ding, K., Wang, A., Boerneke, M.A., Dibrov, S.M., Hermann, T., Aryl-substituted aminobenzimidazoles targeting the hepatitis C virus internal ribosome entry site, *Bioorganic & Medicinal Chemistry Letters* (2014), doi: <http://dx.doi.org/10.1016/j.bmcl.2014.05.009>

This is a PDF file of an unedited manuscript that has been accepted for publication. As a service to our customers we are providing this early version of the manuscript. The manuscript will undergo copyediting, typesetting, and review of the resulting proof before it is published in its final form. Please note that during the production process errors may be discovered which could affect the content, and all legal disclaimers that apply to the journal pertain.

# Aryl-substituted aminobenzimidazoles targeting the hepatitis C virus internal ribosome entry site

Kejia Ding, Annie Wang, Mark A. Boerneke, Sergey M. Dibrov and Thomas Hermann\*

Department of Chemistry and Biochemistry, University of California, San Diego, 9500 Gilman Drive, La Jolla, California 92093, United States

\*Corresponding author: tch@ucsd.edu

## ABSTRACT

We describe the exploration of N1-aryl-substituted benzimidazoles as ligands for the hepatitis C virus (HCV) internal ribosome entry site (IRES) RNA. The design of the compounds was guided by the co-crystal structure of a benzimidazole viral translation inhibitor in complex with the RNA target. Structure-binding activity relationships of aryl-substituted benzimidazole ligands were established that were consistent with the crystal structure of the translation inhibitor complex.

Infection with hepatitis C virus (HCV), which affects over 180 million individuals worldwide, is a major cause of hepatocellular carcinoma and the leading indication for liver transplantation.<sup>1</sup> While two classes of direct antiviral drugs are now available, including protease and polymerase inhibitors,<sup>2, 3</sup> the high genetic variability of HCV poses a constant threat of resistance development and requires the exploration of additional targets for antiviral therapy.<sup>4-6</sup> Since the HCV RNA genome contains several highly conserved *cis*-acting elements that adopt defined structures, the repertoire for antiviral intervention may be expanded to RNA targets. The internal ribosome entry site (IRES) in the 5' untranslated region (UTR) of the viral genome stands out for its high sequence conservation in clinical isolates and serves an essential function for ribosome recruitment and initiation of HCV protein synthesis in infected host cells. We have recently established<sup>7</sup> the subdomain IIa RNA of the HCV IRES as the target for 2-aminobenzimidazole viral translation inhibitors<sup>8</sup> (Figure 1). Benzimidazole scaffolds have been recognized as useful platforms for the synthesis of biologically active ligands for other RNA targets, including RNA loops,<sup>9, 10</sup> the HIV TAR element,<sup>11</sup> microRNAs<sup>12</sup> and RNA repeat motifs.<sup>13, 14</sup> The 2-aminobenzimidazoles inhibit the IRES function by capturing an extended conformation of the IIa RNA target which has been proposed to block translation initiation.<sup>15</sup> A Förster resonance energy transfer (FRET) assay has been developed to monitor the selective conformational capture by ligands and measure their target affinity for the IIa RNA.<sup>7, 16</sup>

Crystal structure analysis of the IIa RNA in complex with the 2-aminobenzimidazole **1** revealed the key interactions responsible for target recognition by the translation inhibitors.<sup>17</sup> Since previous structure-binding activity relationship studies on the 2-aminobenzimidazoles had revealed the importance of a rigid core scaffold for target affinity,<sup>8</sup> we explored N1-aryl-

substituted benzimidazoles (**2**) which also lack the synthetically cumbersome chroman scaffold. The compounds designed here retain the amino-imidazole core required for recognition of the H<sub>2</sub>A RNA and provide a rigid aryl linker for a dimethylamino substituent that participates in interactions with a phosphate group while avoiding an entropic penalty for pre-organization of the dimethylaminopropyl chain in ligands such as **1** (Figure 1B,C). Modeling studies suggested that the twist conformation between the imidazole and aryl ring along with an appropriate *meta*-substitution position for the dimethylamino group would provide a rigid vector for interaction with the phosphate group of residue A109 (Figure 1C).

Here, we describe the synthesis and target affinity testing of several chemical series of N1-aryl-substituted 2-aminobenzimidazoles (Figure 2), including the compounds **3** and the 2-amide derivatives **4**. To evaluate the importance of the 2-amino substituent, we prepared 2-hydroxybenzimidazole analogs **5**. A small number of dimethylaminopropyl-substituted compounds **6** which carried aryl substituents at the benzene ring were included as well.

Synthesis of phenylether derivatives in the series **3**, **4** and **5** ( $R^1 = R^4O$ , Scheme 1 and Table 1) was planned to progress through an N-aryl-substituted *o*-phenylenediamine common intermediate (**12**) which was cyclized to the benzimidazole by reaction with isothiocyanates or phosgene. The intermediate **12** was prepared over three steps from halogen-substituted nitrophenols **7**. Alkylation of **7** yielded phenylethers **9**. The parent phenol **9** ( $R^4 = OH$ ) was obtained as the tert-butyldimethylsilyl (TBDMS) ether derivative. Coupling with anilines **10** followed by reduction of the nitro group furnished the common intermediate **12**. Cyclization of **12** with acetyl or benzoyl isothiocyanates gave the 2-amide derivatives **4** which were further hydrolyzed to the parent 2-aminobenzimidazoles **3**. Treatment of **12** with phosgene yielded 2-hydroxybenzimidazole analogs **5**. Two aniline derivatives in the 1-aryl-2-aminobenzimidazole

series (**3h** and **3i**, Table 1) were synthesized through isothiocyanate cyclization of an intermediate that was obtained by two consecutive Buchwald-Hartwig aminations of 2,4-dichloro-1-nitrobenzene **13** (Scheme 2). The *N,N*-dimethylaminopropyl-substituted benzimidazoles **6** (Table 2) were synthesized following the route outlined in Scheme 3. Dichloronitrobenzene precursors were alkylated to install the dimethylaminopropyl chain. Coupling with aromatic amines or boronic acids led to nitro-aniline (**22**) and -biphenyl (**23**) intermediates which, after reduction, were cyclized with isothiocyanate to furnish the amides **24** whose hydrolysis gave the final products **6**.

The identity of all synthesized compounds from the chemical series **3**, **4**, **5** and **6** was established after column chromatographic purification by mass- and NMR. Crystal structures were determined for selected derivatives, including the 2-aminobenzimidazole **3e**. Compounds were tested for binding to the IRES IIa RNA by triplicate titration in the IIa FRET assay as previously described.<sup>16</sup> Target affinity expressed as EC<sub>50</sub> value was determined from fitting of single-site binding dose response curves to the titration data (Tables 1 and 2). See the Supporting Information for experimental procedures, spectra, crystal structure and FRET titration curves.

Of the nine 1-aryl-2-aminobenzimidazoles **3** synthesized, all but two showed binding to the IIa RNA target with affinities between 74–250  $\mu$ M. Exceptions were the unsubstituted phenol **3a** and the picolyl ether **3d**. Inspection of the binding pocket around **1** in the co-crystal structure suggested that while the parent phenol **3a** is unable to form interactions beyond the amino-imidazole scaffold, in the derivative **3d** the bulky picolyl ether substituent off the 5-position might interfere with ligand docking at the G110 base of the RNA target (Figure 1C). In contrast, the more flexible aliphatic dimethylaminoalkyl ether chain was tolerated at the same position, as attested by the binding of compounds **3b** and **3c** (250 and 210  $\mu$ M, respectively). Improvement

of the affinity by 2-fold was seen in derivative **3e** (95  $\mu$ M) which carried a 5-dimethylaminopropyl ether substituent at the benzimidazole and an additional *p*-dimethylamino group on the imidazole-linked phenyl ring. The same combination of functional groups, however, with the dimethylaminoalkyl ether chain moved to the 6-position reduced binding of compound **3f** (170  $\mu$ M). Relocation of the dimethylamino substituent from the *para*- to the *meta*-position at the imidazole-linked phenyl ring increased binding in derivative **3g** (120  $\mu$ M), yet not to the level of **3e**. Finally, aromatic substituents were tolerated at the benzimidazole 6-position as indicated by the affinity of compounds **3h** and **3i**, which were among the most active ligands synthesized here (74 and 100  $\mu$ M, respectively). In comparison, compounds **6h** and **6i** which carried the same aromatic pyridine substituents at the 6-position but had the *m*-dimethylaminophenyl ring at the imidazole replaced with a flexible dimethylaminopropyl chain showed weaker target affinity (both, 160  $\mu$ M). Attachment of a *m*-dimethylaminophenyl group at the 7-position of the benzimidazole retained binding in compound **6j** albeit only at 290  $\mu$ M.

The crystal structure of compound **3e** (see Supporting Information) shows a twist angle of 67° between the imidazole and the phenyl ring attached at the 1-position. As a consequence, a good fit of the 1-phenyl ring in **3e** and the dimethylaminopropyl chain in **1** bound to the Ila RNA target was observed in a superposition of the two compounds (Figure 3). The *meta* position of the phenyl ring in **3e** is pointing at the location of the dimethylamino group in **1** which forms a key hydrogen bond with the phosphate of A109 in the RNA target (Figures 1C and 3B). Comparison of the derivatives **3f** and **3g** suggests that higher affinity is achieved by substitution of the phenyl ring with a dimethylamino group at the *meta* position compared to the *para* position. In the superposition of **3e** on the **1** target complex, the dimethylaminopropyl ether chain at the benzimidazole 5-position is directed towards a cleft lined by the sugar phosphate backbone

of residues A54-U56 (Figure 3B). This region is located in a flexible internal loop of the IIa RNA target (Figure 1A) and undergoes a large conformational change upon binding of the ligand **1**. Such adaptive binding might allow the accommodation of flexible substituents at the benzimidazole 5-position, for example, the dimethylaminopropyl ether chain in the **3e** derivative. However, as indicated by the inactivity of compound **3d**, which carries a picolyl ether substituent, bulky and more rigid groups at the 5-position may not be reconciled with target adaptation.

Acylation of the 2-amino group abolished binding as indicated by compounds in the series **4**. The acetylated derivative **4ba** was an exception for which a target affinity of 100  $\mu\text{M}$  was measured, surpassing that of the parent compound **3b** (250  $\mu\text{M}$ ). This observation is not readily reconciled with the crystal structure of the ligand **1** RNA complex, perhaps suggesting that compound **4ba** accesses an alternative binding mode at the target. Nonspecific binding interactions might also be responsible for the strong precipitating properties of the hydroxybenzimidazoles **5**. All tested compounds in this series led to rapid fluorescence quenching in the FRET assay at micromolar concentration, apparently due to precipitation of the dye labeled RNA target.

Here, we have explored N1-aryl-substituted 2-amino-benzimidazoles (**2**) as ligands for the IIa RNA target in the HCV IRES element. Synthesis and affinity testing of several chemical series allowed us to establish structure-binding relationships of the ligands (Figure 4). The observed pattern of compound activity in the FRET target binding assay was readily explained in the context of an earlier determined crystal structure of benzimidazole **1** bound to the IIa RNA. Ligands with the highest affinity showed binding at EC50 values around 74–100  $\mu\text{M}$  which is inferior to the previously studied tricyclic benzimidazoles such as **1**. Given the more facile

synthetic accessibility of the chemical series **2**, in combination with guidance from the clear structure-binding activity relationship established in the current work, we will explore further optimization of the N1-aryl-substituted benzimidazoles in the future.

### Acknowledgments

This work was supported by the National Institutes of Health (grant No. AI72012). Support of the NMR facility by the National Science Foundation is acknowledged (CRIF grant CHE-0741968).

### References

1. Thomas, D. L. *Nat. Med.* **2013**, *19*, 850.
2. Pawlotsky, J. M. *Adv. Pharmacol.* **2013**, *67*, 169.
3. Manns, M. P.; von Hahn, T. *Nat. Rev. Drug. Discov.* **2013**, *12*, 595.
4. Scheel, T. K.; Rice, C. M. *Nat. Med.* **2013**, *19*, 837.
5. Salvatierra, K.; Fareleski, S.; Forcada, A.; Lopez-Labrador, F. X. *World. J. Virol.* **2013**, *2*, 6.
6. Bartenschlager, R.; Lohmann, V.; Penin, F. *Nat. Rev. Microbiol.* **2013**, *11*, 482.
7. Parsons, J.; Castaldi, M. P.; Dutta, S.; Dibrov, S. M.; Wyles, D. L.; Hermann, T. *Nat. Chem. Biol.* **2009**, *5*, 823.
8. Seth, P. P.; Miyaji, A.; Jefferson, E. A.; Sannes-Lowery, K. A.; Osgood, S. A.; Propp, S. S.; Ranken, R.; Massire, C.; Sampath, R.; Ecker, D. J.; Swayze, E. E.; Griffey, R. H. *J. Med. Chem.* **2005**, *48*, 7099.
9. Velagapudi, S. P.; Pushechnikov, A.; Labuda, L. P.; French, J. M.; Disney, M. D. *ACS Chem. Biol.* **2012**, *7*, 1902.
10. Velagapudi, S. P.; Seedhouse, S. J.; French, J.; Disney, M. D. *J. Am. Chem. Soc.* **2011**, *133*, 10111.
11. Ranjan, N.; Kumar, S.; Watkins, D.; Wang, D.; Appella, D. H.; Arya, D. P. *Bioorg. Med. Chem. Lett.* **2013**, *23*, 5689.



12. Velagapudi, S. P.; Gallo, S. M.; Disney, M. D. *Nat. Chem. Biol.* **2014**, *10*, 291.
13. Parkesh, R.; Childs-Disney, J. L.; Nakamori, M.; Kumar, A.; Wang, E.; Wang, T.; Hoskins, J.; Tran, T.; Housman, D.; Thornton, C. A.; Disney, M. D. *J. Am. Chem. Soc.* **2012**, *134*, 4731.
14. Childs-Disney, J. L.; Hoskins, J.; Rzuczek, S. G.; Thornton, C. A.; Disney, M. D. *ACS Chem. Biol.* **2012**, *7*, 856.
15. Dibrov, S. M.; Parsons, J.; Carnevali, M.; Zhou, S.; Ryneerson, K. D.; Ding, K.; Garcia Segal, E.; Brunn, N. D.; Boerneke, M. A.; Castaldi, M. P.; Hermann, T. *J. Med. Chem.* **2013**.
16. Zhou, S.; Ryneerson, K. D.; Ding, K.; Brunn, N. D.; Hermann, T. *Bioorg. Med. Chem.* **2013**, *21*, 6139.
17. Dibrov, S. M.; Ding, K.; Brunn, N. D.; Parker, M. A.; Bergdahl, B. M.; Wyles, D. L.; Hermann, T. *Proc. Natl. Acad. Sci. U. S. A.* **2012**, *109*, 5223.

## Figure Legends

**Figure 1.** Ligand design for the internal ribosome entry site (IRES) target of hepatitis C virus (HCV). A) The IRES element comprises the first 342 nucleotides in the 5' untranslated region (UTR) of the HCV RNA genome. The boxed region highlights the subdomain IIa target whose secondary structure is shown in on the right. B) Structures of a 2-aminobenzimidazole translation inhibitor **1** which was previously co-crystallized in complex with the subdomain IIa RNA, and aryl-substituted 2-aminobenzimidazoles **2** which were designed using guidance by the co-crystal structure of the IIa RNA in complex with **1**. C) Model of the 1-phenyl-2-aminobenzimidazole core of **2** (light blue) docked at the binding site of **1** (yellow) in the subdomain IIa RNA co-crystal structure.<sup>17</sup> Hydrogen bonds and nucleotides participating in intramolecular contacts are indicated.

**Figure 2.** Benzimidazole derivatives for targeting the HCV IRES subdomain IIa RNA: 1-aryl-2-aminobenzimidazoles **3**, 1-aryl-2-acylaminobenzimidazoles **4**, 1-aryl-2-hydroxybenzimidazoles **5**, *N,N*-dimethylaminopropyl-substituted benzimidazoles **6**. Compounds made in each series are shown in Tables 1 and 2.

**Figure 3.** A) Crystal structure of compound **3e** (see Supporting Information, CCDC deposit number 978337). Hydrogen atoms are not shown. The dihedral twist angle between the imidazole and dimethylaniline rings is indicated. B) Model of the compound **3e** crystal structure (light blue) superimposed on the HCV translation inhibitor **1** (yellow) in the subdomain IIa RNA co-crystal structure.<sup>17</sup> Hydrogen bonds and nucleotides participating in intramolecular contacts

are indicated. Residues G52 and A53, which stack below and above the ligand are shown transparent.

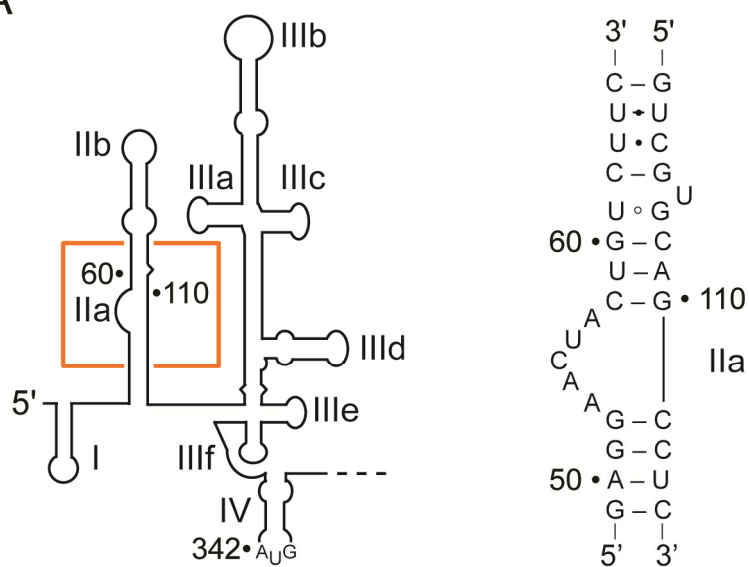
**Figure 4.** Structure-binding activity relationships discovered for 1-aryl-2-aminobenzimidazoles targeting the HCV IRES subdomain IIa RNA.

**Scheme 1.** Synthesis of 1-aryl-2-aminobenzimidazoles **3**, 1-aryl-2-acylaminobenzimidazoles **4** and 1-aryl-2-hydroxybenzimidazoles **5** from halo-nitrophenols **6**. Preparation of 5-substituted benzimidazoles commenced from 4-chloro-3-nitrophenol (X=Cl), that of 6-substituted products from 3-fluoro-4-nitrophenol (X=F). Reagents and conditions: a) (for R<sup>4</sup>=H, **8**=TBDMSCl) K<sub>2</sub>CO<sub>3</sub>, ACN, reflux, 2.5-28 h, 52-94 % yield; b) Cs<sub>2</sub>CO<sub>3</sub>, Pd<sub>2</sub>(dba)<sub>3</sub>, (±)BINAP, 19-28 h, 31-91 % yield; c) K<sub>2</sub>CO<sub>3</sub>, ACN, reflux, 21-41 h, 34-36 % yield; d) H<sub>2</sub> (1 atm), Pd/C or PtO<sub>2</sub>, MeOH, RT, 1.5-25 h; e) acylNCS (acyl=acetyl or benzoyl), DIPC, DIPEA, ACN, 22-48 h, 20-66 % yield over two steps; f) phosgene (20 % in toluene), pyridine, DCM, RT, 3-24 h, 50-64 % yield two steps; g) 1N HCl, H<sub>2</sub>O, dioxane, reflux, 18-28 h, 27-96 % yield. Abbreviations: TBDMSCl = tert-butyldimethylsilyl chloride; ACN = acetonitrile; dba = dibenzylideneacetone; BINAP = 2,2'-bis(diphenylphosphino)-1,1'-binaphthalene; RT = room temperature; DIPC = N,N'-diisopropylcarbodiimide; DIPEA = N,N-diisopropylethylamine; DCM = dichloromethane.

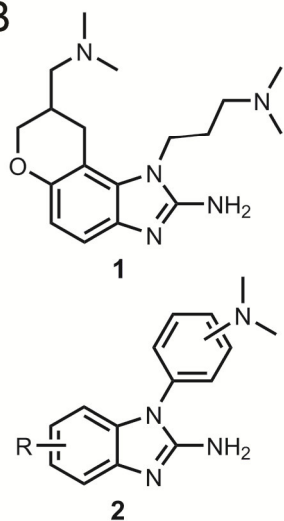
**Scheme 2.** Synthesis of 1-aryl-2-aminobenzimidazoles **3h** and **3i**. Reagents and conditions: ba) Cs<sub>2</sub>CO<sub>3</sub>, Pd<sub>2</sub>(dba)<sub>3</sub>, (±)BINAP, toluene, reflux, 21 h, 43 % yield, two steps; **14** was synthesized from N,N-dimethyl-3-nitroaniline by reduction with H<sub>2</sub> (1 atm), Pd/C in MeOH, 20 hr; bb) Cs<sub>2</sub>CO<sub>3</sub>, Pd<sub>2</sub>(dba)<sub>3</sub>, (±)BINAP, dioxane, reflux, 20-44 h, 34-43 % yield d) H<sub>2</sub> (1 atm), Pd/C or PtO<sub>2</sub>, MeOH, RT, 21-23 h; e) benzoylNCS, DIPC, DIPEA, ACN, 24-26 h, 22-32 % yield over two steps; g) 1N HCl, H<sub>2</sub>O, dioxane, reflux, 23-26 h, 27-56 % yield.

**Scheme 3.** Synthesis of *N,N*-dimethylaminopropyl-substituted benzimidazoles **6** from dichloro-nitrobenzenes **13**. Preparation of 6-substituted benzimidazoles commenced from 1,2-dichloro-4-nitrobenzene, that of 7-substituted products from 1,2-dichloro-3-nitrobenzene. Reagents and conditions: a)  $K_2CO_3$ , ACN, reflux, 24 h, 96-97 % yield; b)  $Cs_2CO_3$ ,  $Pd_2(dba)_3$ , ( $\pm$ )BINAP, 19-23 h, 37-80 % yield range; d)  $H_2$  (1 atm), Pd/C or  $PtO_2$ , MeOH, RT, 21-25 h; e) benzoylNCS, DIPC, DIPEA, ACN, 19-21 h, 29-33 % yield over two steps; g) 1N HCl,  $H_2O$ , dioxane, reflux, 17-21 h, 22-46 % yield.

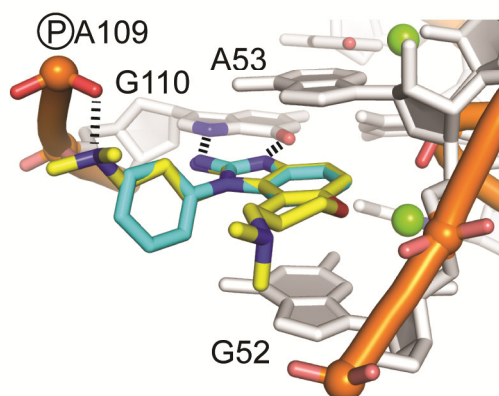
A

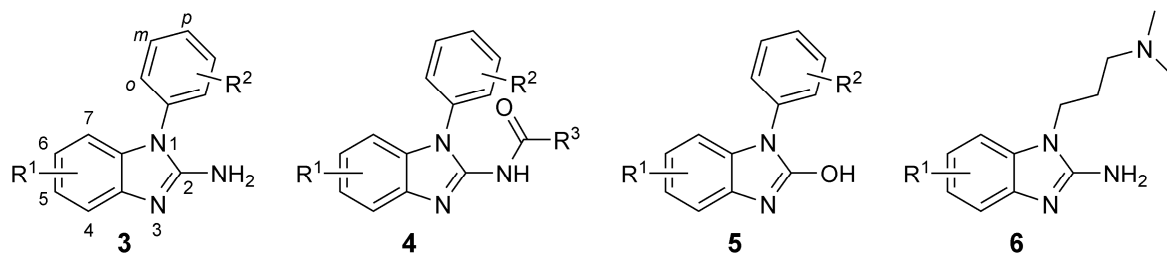


B

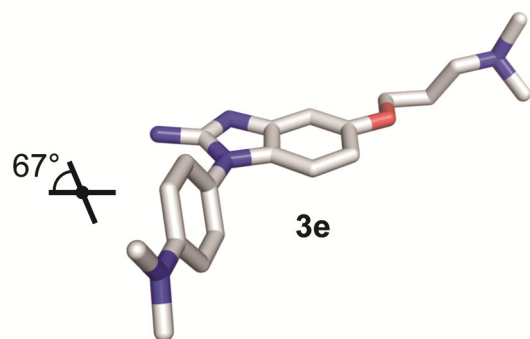


C

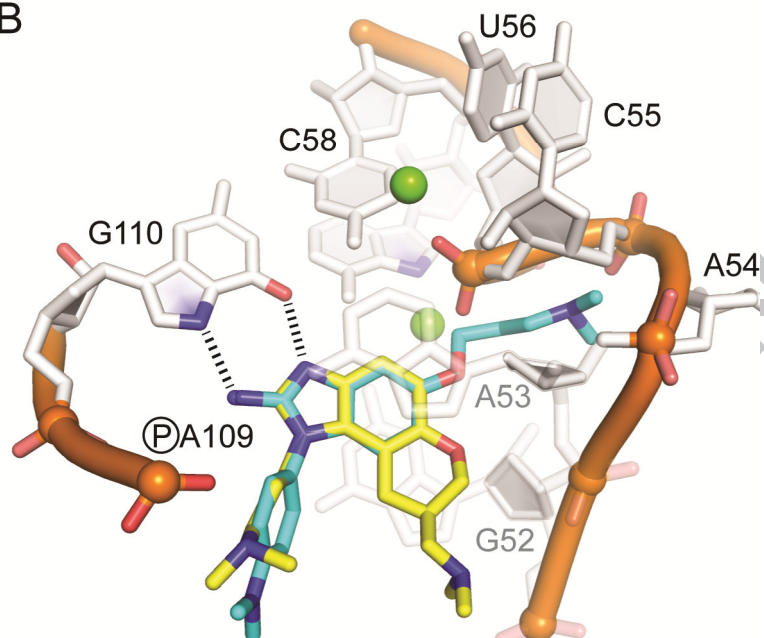




A



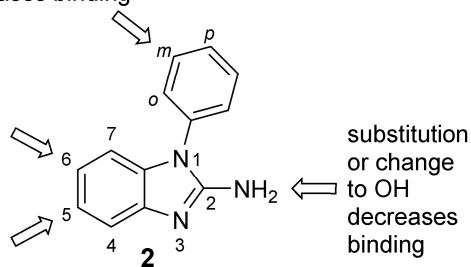
B



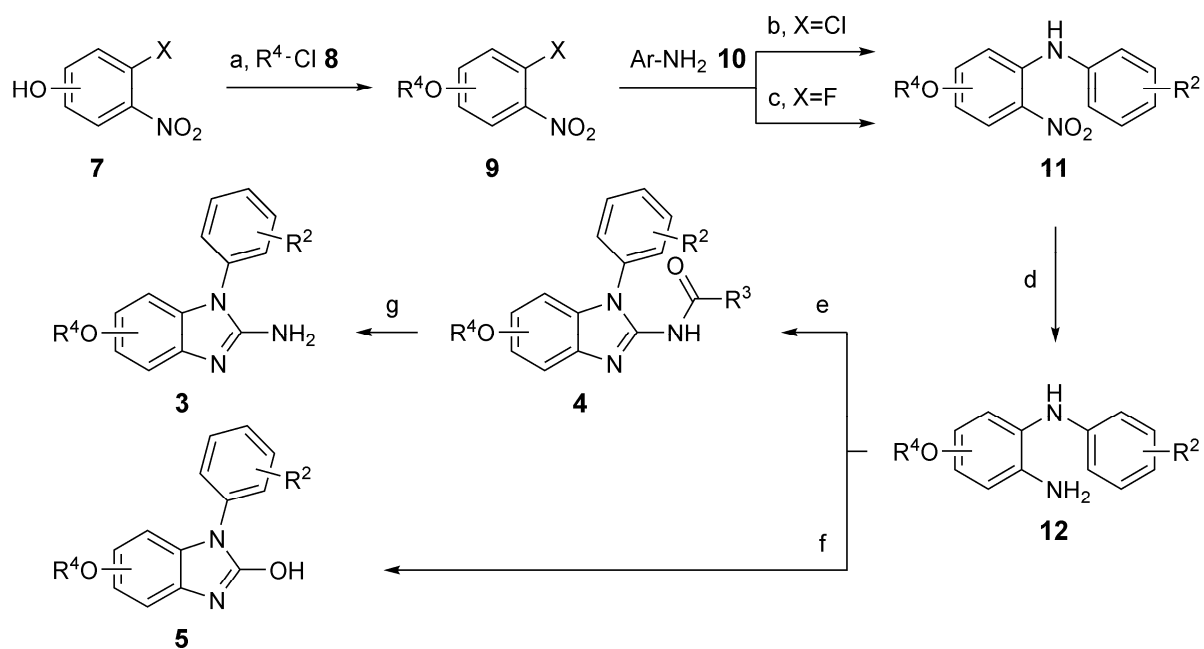
(CH<sub>3</sub>)<sub>2</sub>N at *meta* position increases binding

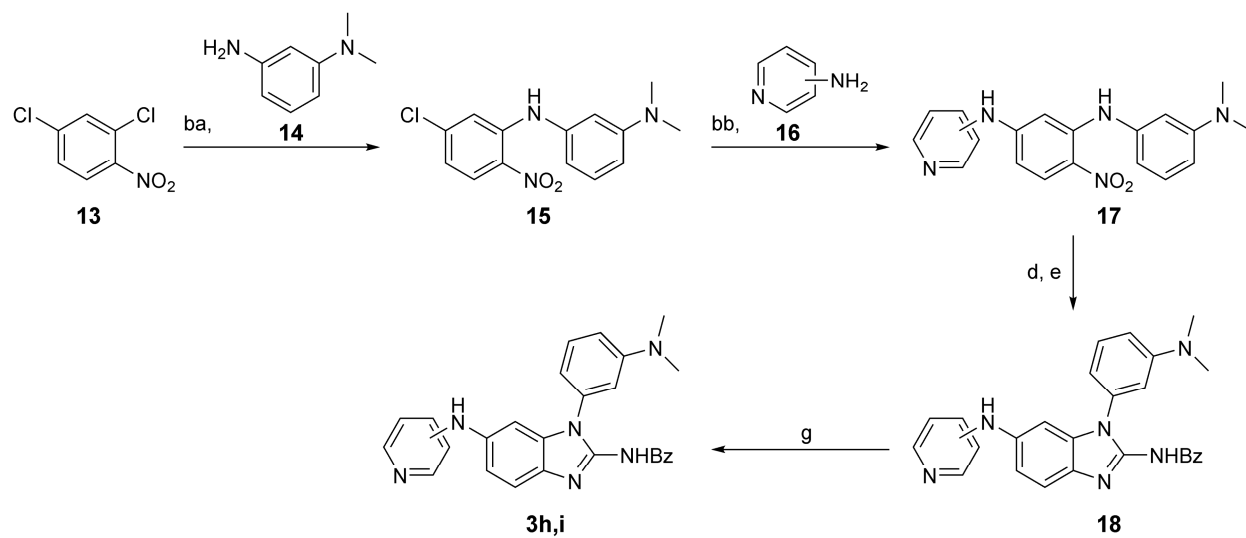
aromatic substituent linked  
via CH<sub>2</sub> or NH beneficial

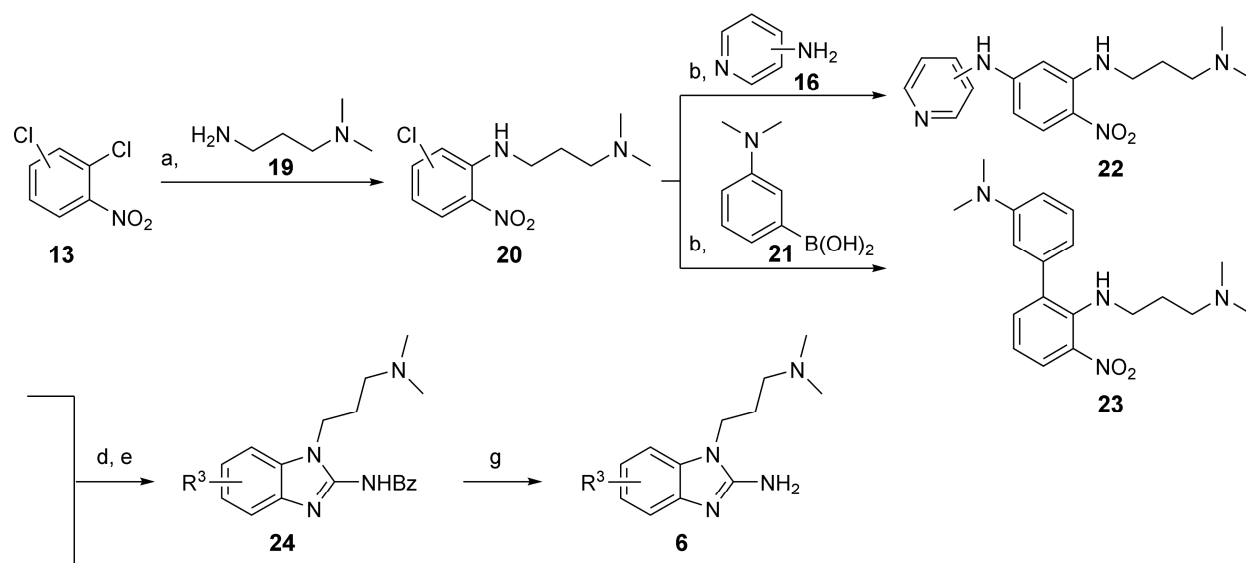
flexible substituent with polar  
end group increases binding









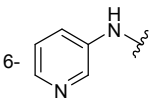
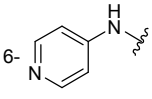
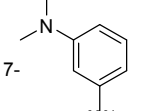


**Table 1.** Activity of 1-aryl-benzimidazole derivatives **3**, **4** and **5** in the FRET assay.

Compound	R <sup>1</sup>	R <sup>2</sup>	R <sup>3</sup>	EC <sub>50</sub> [μM] <sup>a</sup>
<b>3a</b>	5-OH	H	H	n.a.
<b>3b / 5b</b>		H	H	250 ± 66
<b>3c / 5c</b>		H	H	210 ± 39
<b>3d</b>		H	H	n.a.
<b>3e</b>			H	95 ± 6
<b>3f / 5f</b>			H	170 ± 16
<b>3g</b>			H	120 ± 5
<b>3h</b>			H	74 ± 2
<b>3i</b>			H	100 ± 12
<b>4ba</b>		H	CH <sub>3</sub>	100 ± 13
<b>4ca</b>		H	CH <sub>3</sub>	> 500
<b>4ab</b>	5-OH	H	C <sub>6</sub> H <sub>5</sub>	n.a.
<b>4bb</b>		H	C <sub>6</sub> H <sub>5</sub>	> 500
<b>4cb</b>		H	C <sub>6</sub> H <sub>5</sub>	> 500
<b>4eb</b>			C <sub>6</sub> H <sub>5</sub>	precip.
<b>4fb</b>			C <sub>6</sub> H <sub>5</sub>	precip.

<sup>a</sup>EC<sub>50</sub> values (± standard error from triplicate experiments) are shown for 2-aminobenzimidazoles **3** and acyl derivatives **4**. All tested 2-hydroxybenzimidazoles **5** precipitated RNA at a concentration between 50-100 μM.

**Table 2.** Activity of *N,N*-dimethylaminopropyl-substituted benzimidazoles **6** in the FRET assay.

Compound	R <sup>1</sup>	EC <sub>50</sub> [ $\mu$ M] <sup>a</sup>
<b>6h</b>		160 $\pm$ 15
<b>6i</b>		160 $\pm$ 29
<b>6j</b>		290 $\pm$ 100

<sup>a</sup>EC<sub>50</sub> values are shown  $\pm$  standard error from triplicate experiments.

HCV IRES

